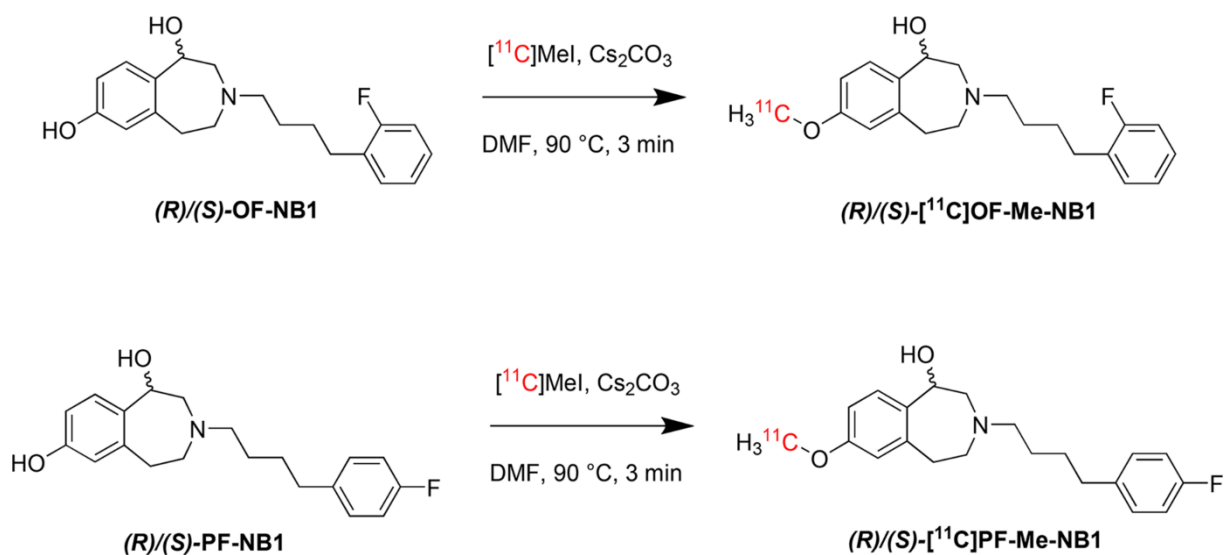
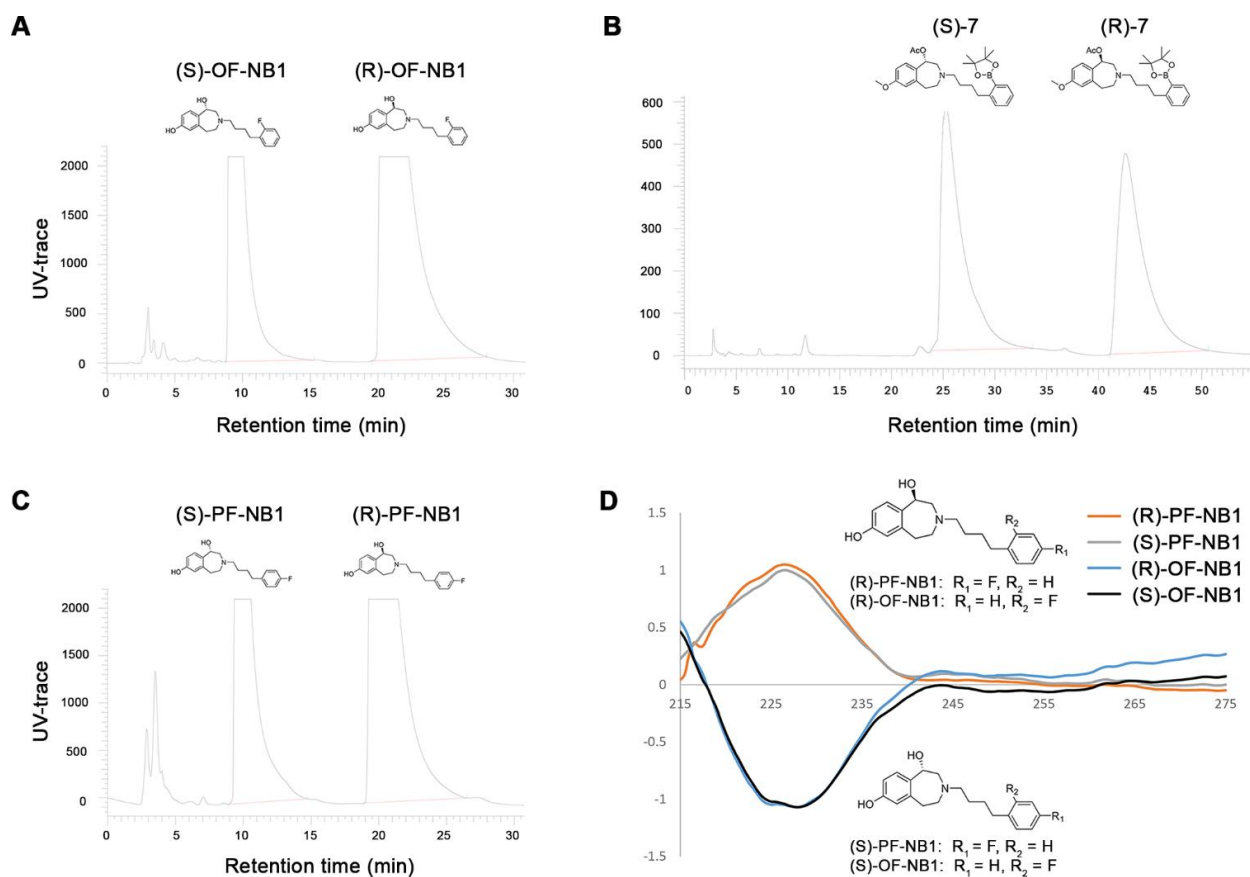


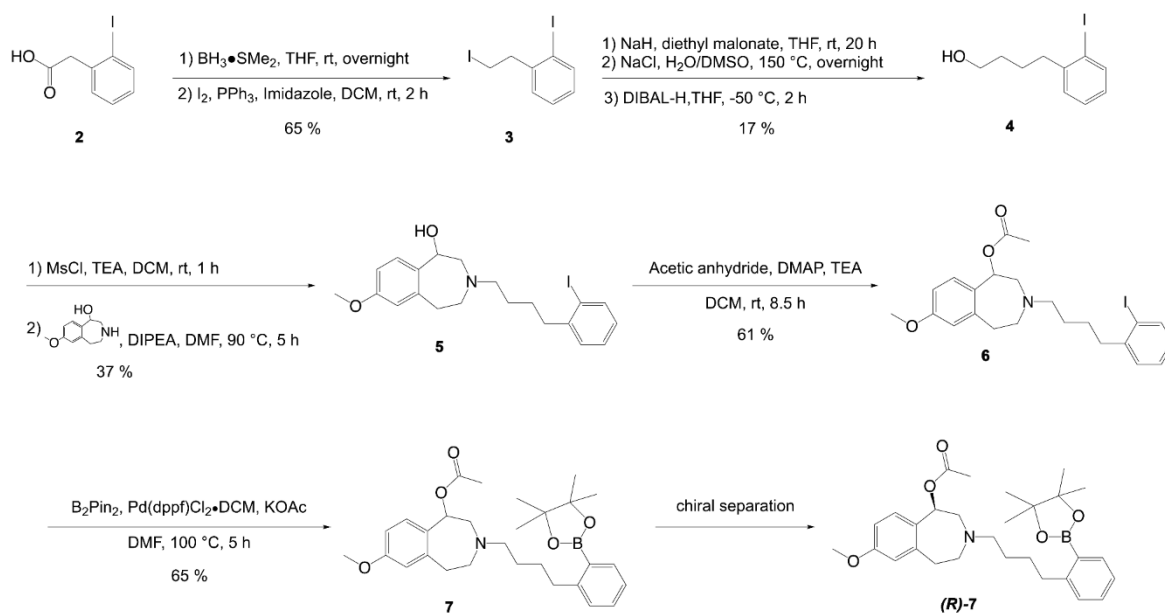
**Supplemental Figure 1:** Synthesis of reference compounds OF-Me-NB1 and PF-Me-NB1 as well as the respective phenolic precursors OF-NB1 and PF-NB1. Chiral separation was carried out by semipreparative HPLC under isochratic normal phase conditions using a system of hexane/isopropanol (4:1). Experimental procedures, NMR data and high-resolution mass spectrometry can be found at the following link: <https://www.research-collection.ethz.ch/handle/20.500.11850/266284>.



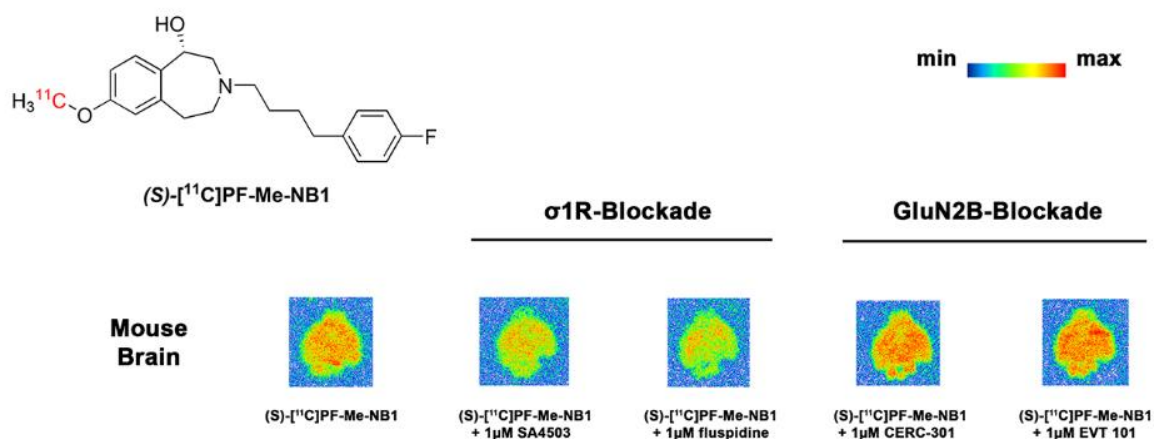
**Supplemental Figure 2:** Radiosynthesis of  $(R)$ - $^{11}\text{C}$ -PF-Me-NB1,  $(S)$ - $^{11}\text{C}$ -PF-Me-NB1,  $(R)$ - $^{11}\text{C}$ -OF-Me-NB1 and  $(S)$ - $^{11}\text{C}$ -OF-Me-NB1.



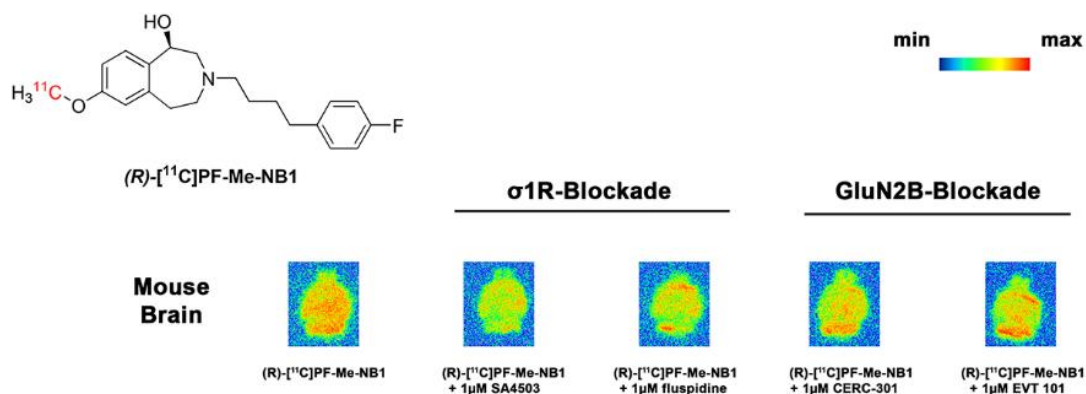
**Supplemental Figure 3:** Chiral resolution and circular dichroism spectra. **A.** Chiral resolution of precursor OF-NB1. **B.** Chiral resolution of precursor PF-NB1. **C.** Chiral resolution of aryl boronic ester precursor **7**. **D.** Circular dichroism spectra of (*R*)- and (*S*)-PF-NB1 as well as (*R*)- and (*S*)-OF-NB1.



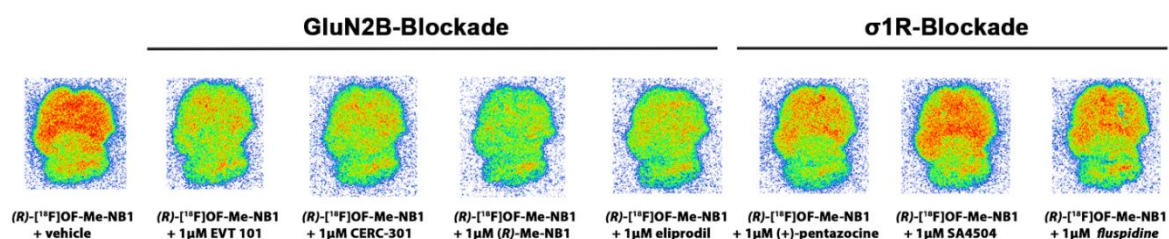
**Supplemental Figure 4:** Synthesis of aryl boronic ester precursor **7** for radiofluorination. Chiral separation was carried out by semipreparative HPLC under isocratic normal phase conditions using a system of hexane/isopropanol (98:2). Experimental procedures, NMR data and high-resolution mass spectrometry can be found at the following link link: <https://www.research-collection.ethz.ch/handle/20.500.11850/266284>.



**Supplemental Figure 5:** Representative *in vitro* autoradiogram of (S)-<sup>11</sup>C-PF-Me-NB1 on coronal mouse brain sections. GluN2B ligands (CERC-301, EVT 101) and σ1R ligands (SA4503, fluspidine) were used to assess GluN2B-specificity and selectivity over the σ1R.



**Supplemental Figure 6:** Representative *in vitro* autoradiogram of (R)-<sup>11</sup>C-PF-Me-NB1 on coronal mouse brain sections. GluN2B ligands (CERC-301 and EVT 101) as well as σ1R ligands (SA4503 and fluspidine) were used to assess GluN2B-specificity and selectivity over the σ1R.



**Supplemental Figure 7:** Representative *ex vivo* autoradiography at 30 min post injection of (R)-<sup>18</sup>F-OF-Me-NB1 and subsequent *in vitro* displacement by GluN2B ligands (EVT-101, CERC-301, (R)-Me-NB1 and eliprodil) and σ1 receptor ligands ((+)-pentazocine, SA4503 and fluspidine). Conventional *in vivo* specificity and selectivity evaluation of PET radioligands is carried out by the injection of non-radioactive blockers in combination with the radioligand to test. This strategy, however, is hampered by different confounders such as unfavourable pharmacokinetic properties and metabolism of the blocker. For biological targets located in the central nervous system, there is an evident prerequisite for the blocker to cross the blood-brain barrier in order to exhibit an efficient blockade. Furthermore, potential off-target binding of blocker metabolites as well as the complexity of neuronal signalling systems (eg. receptor crosstalk) can ultimately lead to false conclusions on tracer specificity and selectivity. To avoid such confounders, we performed an *ex vivo* autoradiography of (R)-<sup>18</sup>F-OF-Me-NB1 in Wistar rats and subsequently treated the brain slices with different displacer *in vitro*. *Ex vivo* autoradiographic brain slices were treated with GluN2B antagonists EVT 101, CERC-301, R-Me-NB1 and eliprodil as well as σ1 receptor ligands (+)-pentazocine, SA4503 and fluspidine. Radioligand displacement occurred upon addition of all tested GluN2B-antagonists.

**Supplemental Table 1:** Organ biodistribution of (*R*)-<sup>18</sup>F-OF-Me-NB1 in Wistar rats (n=4), reported as averaged % normalized injected dose per gram body weight ± SD.

<i>organ</i>	<i>30 min post injection</i>	<i>30 min post injection + eliprodil 2 mg/kg</i>	<i>specificity %</i>
<i>spleen</i>	0.24 ± 0.01	0.19 ± 0.02	22
<i>liver</i>	0.31 ± 0.04	0.20 ± 0.03	37
<i>kidney</i>	0.58 ± 0.11	0.20 ± 0.04	66
<i>adrenal gland</i>	1.9 ± 0.5	0.33 ± 0.07	83
<i>lung</i>	0.24 ± 0.02	0.28 ± 0.05	no specificity
<i>femur</i>	0.067 ± 0.017	0.052 ± 0.001	22
<i>heart</i>	0.047 ± 0.004	0.060 ± 0.006	no specificity
<i>fat</i>	0.056 ± 0.024	0.047 ± 0.008	16
<i>intestine</i>	0.65 ± 0.08	0.91 ± 0.08	no specificity
<i>testicle</i>	0.093 ± 0.001	0.068 ± 0.009	27
<i>blood</i>	0.010 ± 0.000	0.043 ± 0.059	no specificity
<i>urine</i>	0.45 ± 0.17	0.80 ± 0.61	no specificity
<i>muscle</i>	0.059 ± 0.006	0.066 ± 0.010	no specificity
<i>pancreas</i>	0.59 ± 0.09	0.21 ± 0.04	64
<i>skin</i>	0.059 ± 0.008	0.061 ± 0.009	no specificity



**Supplemental Table 2:** Regional biodistribution of (R)-<sup>18</sup>F-OF-Me-NB1 in the Wistar rat brain (n=4), reported as averaged % normalized injected dose per gram body weight ± SD.

<i>brain region</i>	<i>30 min post injection</i>	<i>30 min post injection + eliprodil 2 mg/kg</i>	<i>specificity %</i>
<i>olfactory bulb</i>	0.16 ± 0.02	0.09 ± 0.00	47
<i>hippocampus</i>	0.20 ± 0.02	0.11 ± 0.01	44
<i>thalamus</i>	0.20 ± 0.02	0.12 ± 0.01	38
<i>cerebellum</i>	0.15 ± 0.01	0.09 ± 0.00	40
<i>brain stem</i>	0.22 ± 0.02	0.10 ± 0.00	53
<i>colliculus superior/inferior</i>	0.20 ± 0.02	0.094 ± 0.006	53
<i>cortex</i>	0.20 ± 0.02	0.10 ± 0.01	50
<i>striatum</i>	0.19 ± 0.02	0.10 ± 0.01	46